UC Riverside

UC Riverside Previously Published Works

Title

Integrated InSAR, 3D volumetric inversion, and deep learning reveal ongoing oil induced subsidence in the East Coast of Lake Maracaibo

Permalink

https://escholarship.org/uc/item/2841s1zm

Journal

Revista de Teledetección, issue 69

ISSN

1133-0953

Authors

Quintana-Sánchez, Gabriela
Reinoza-Gómez, Carlos E
Audemard, Franck A
et al.

Publication Date

2026-11-16

DOI

10.4995/raet.2027.26485

Copyright Information

This work is made available under the terms of a Creative Commons Attribution License, available at https://creativecommons.org/licenses/by/4.0/

Peer reviewed

eScholarship.org Powered by the California Digital Library
University of California

Recibido: 14/06/2026
Aceptado: 27/10/2026
Disponible en línea: 13/11/2026
Publicado: 31/01/2027

Crossref
Similarity Check
Powered by iThenticate

REVISTA DE TELEDETECCIÓN
Asociación Española de Teledetección
(2026) 69, e26845
EISSN 1988-8740
https://doi.org/10.4995/raet.2027.26845

Integrated InSAR, 3D volumetric inversion, and deep learning reveal ongoing oil induced subsidence in the East Coast of Lake Maracaibo

Gabriela Quintana-Sánchez[1*], Carlos E. Reinoza-Gómez[2], Franck A. Audemard[2,3], Fikret Dogru[4], Gareth Funning[5], Fredy Díaz-Mila[6]

[1] *Central University of Venezuela (UCV). Venezuelan Foundation for Seismological Research (FUNVISIS), Venezuela.*
[2] *Center for Scientific Research and Higher Education of Ensenada, Baja California, México.*
[3] *Central University of Venezuela (UCV) Faculty of Engineering, School of Geology, Mines and Geophysics, Venezuela.*
[4] *Ataturk University, Oltu Vocational College, Construction, Erzurum, Turkey. ORCID:*
[5] *University of California, Riverside, USA.*
[6] *Colombian Geological Survey - District University of Bogotá, Colombia.*

Highlights

- SBAS-DInSAR, 3D inversion, and LSTM integrated to assess COLM subsidence.
- High subsidence rates with vertical deformation up to −7.1 cm/yr in Lagunillas.
- 3D inversion locates −600 µstrain/yr volumetric strain at ~1,676 m depth.
- LSTM forecasts continued nonlinear subsidence of ~−4 cm/yr through 2027.

Abstract: This study integrates Differential Interferometric Synthetic Aperture Radar (DInSAR) using the Small Baseline Subset (SBAS) approach, 3D volumetric inversion (DTerrain), and Long Short-Term Memory (LSTM) neural networks to quantify and forecast land subsidence along the East Coast of Lake Maracaibo (COLM), Venezuela. We processed a dataset of 280 Sentinel-1 images (2018–2022) to derive high-resolution deformation time series. Line of sight (LOS) velocities indicate significant subsidence rates, reaching −5.91 ± 0.10 cm/yr in Lagunillas and −7.19 ± 0.29 cm/yr in Bachaquero. Decomposition into vertical and horizontal components reveals dominant vertical deformation, with maximum rates of −7.1 cm/yr in Lagunillas. The DTerrain inversion model identifies volumetric strain concentrations at approximately 1676 m depth, consistent with reservoir compaction processes associated with hydrocarbon extraction. The estimated strain values (−600 µstrain/yr) for Lagunillas oilfield suggest significant porosity reduction within Miocene reservoir units. Additionally, the LSTM based forecasting model captures the nonlinear temporal evolution of subsidence, projecting continued deformation at rates of approximately −4 cm/yr through 2027 under current conditions. These results confirm the persistence of subsidence in COLM and highlight its strong linkage to reservoir subsidence. The integrated methodology provides a robust framework for geomechanical monitoring and risk assessment, with direct implications for infrastructure stability and flood hazard mitigation in subsidence prone coastal environments.

Keywords: subsidence, oil extraction, InSAR, modelling, COLM, Venezuela.

To cite this article: Quintana-Sánchez, G., Reinoza-Gómez, C.E., Audemard, F.A., Dogru, F., Funning, G., Díaz-Mila, F. 2026. Integrated InSAR, 3D volumetric inversion, and deep learning reveal ongoing oil induced subsidence in the East Coast of Lake Maracaibo. *Revista de Teledetección*, *69*, e26845. https://doi.org/10.4995/raet.2027.26845

** Corresponding author: gabrielaquintana77@gmail.com*

Asociación Española de Teledetección | Universitat Politècnica de València

Attribution-NonCommercial-ShareAlike 4.0 International (CC BY-NC-SA 4.0)

Integración de InSAR, inversión volumétrica 3D y aprendizaje profundo revelan subsidencia activa inducida por la extracción petrolera en la Costa Oriental del Lago de Maracaibo

Resumen: Este estudio integra el Radar de Apertura Sintética de Interferometría Diferencial (DInSAR), utilizando el enfoque de Subconjunto de Línea Base Pequeña (SBAS), inversión volumétrica 3D (DTerrain) y redes neuronales de Memoria a Corto y Largo Plazo (LSTM), para cuantificar y pronosticar la subsidencia del terreno en la Costa Oriental del Lago de Maracaibo (COLM), Venezuela. Se procesó un conjunto de datos de 280 imágenes de Sentinel-1 (2018–2022) para derivar series temporales de deformación de alta resolución. Las velocidades en la línea de visión (LOS) indican tasas de subsidencia significativas, alcanzando −5,91 ± 0,10 cm/año en Lagunillas y −7,19 ± 0,29 cm/año en Bachaquero. La descomposición en componentes verticales y horizontales revela una deformación vertical dominante, con tasas máximas de −7,1 cm/año en Lagunillas. El modelo de inversión DTerrain identifica concentraciones de deformación volumétrica a una profundidad aproximada de 1676 m, lo cual es consistente con los procesos de compactación de yacimientos asociados a la extracción de hidrocarburos. Los valores de deformación estimados (−600 µstrain/año) para el campo Lagunillas sugieren una reducción significativa de la porosidad dentro de las unidades de yacimientos del Mioceno. Además, el modelo de pronóstico basado en LSTM captura con éxito la evolución temporal no lineal de la subsidencia, proyectando una deformación continua a tasas de aproximadamente −4 cm/año hasta el 2027 bajo las condiciones actuales. Estos resultados confirman la persistencia de la subsidencia en la COLM y resalta su fuerte vínculo con la subsidencia de los yacimientos. La metodología integrada proporciona un marco sólido para el monitoreo geomecánico y la evaluación de riesgos, con implicaciones directas para la estabilidad de la infraestructura y la mitigación de los peligros de inundación en entornos costeros propensos a la subsidencia.

Palabras clave: subsidencia, extracción de hidrocarburos, InSAR, modelado, COLM, Venezuela.

1. Introduction

Land subsidence induced by fluid extraction is a major geomechanical hazard with worldwide implications. Reducing pore pressure within reservoir formations increases effective stress, leading to compaction of porous media and subsequent surface deformation. This process is well documented across major hydrocarbon basins, where cumulative subsidence exceeding several meters has severely compromised infrastructure, coastal defense earthworks, and urban settlements (Murria, 1991; Finol & Sancevic, 1995; Galloway et al., 2011).

Anthropogenic subsidence has been observed worldwide. For example, in the Wilmington Oil Field in Long Beach, California, USA, subsidence has reached 9 m since 1926. This caused significant damage to docks, pipelines, buildings, streets, bridges, and oil wells, requiring extensive repairs to prevent flooding (Mayuga and Allen, 1969). In the Bogotá Savannah, Colombia, the extraction of water from aquifers is one of the main causes of the drop in the phreatic zone, reflecting negative vertical displacements, where a vertical displacement rate of up to 12 cm/yr has been estimated by applying Interferometric Synthetic Aperture Radar —InSAR— techniques (Díaz-Mila et al., 2025). Mexico City, due to the intensive extraction of groundwater, is another example to mention, affecting its urban areas, being the object of study since the decade of the 90s and with current monitoring applying techniques such as GNSS and InSAR, managing to estimate a value of −23 mm/yr of subsidence (Solano-Rojas et al., 2015).

As a Venezuelan example, there is the subsidence of the East Coast of Lake Maracaibo, an administrative subregion of the state of Zulia, western Venezuela, which is home to three well-known oil fields that are not very deep (300 to 1000 m) in the country, such as Tia Juana, Lagunillas, and Bachaquero. The East Coast of Lake Maracaibo (COLM), formerly known as Campos Costanero Bolívar (CCB), was discovered in 1914, with Mene Grande as its first oil field. According to Finol & Sancevic (1995), COLM stretches 55 km, from the northern end of Tía Juana to the southern boundary of Bachaquero, reaching its greatest width at Bachaquero (25 km).

The estimated accumulated subsidence maximum ranges, according to diverse study, from up to −5.03 m (Murria, 1991), up to −5.3 m (Murria

and Saab, 1992), up to −5.013 m, the lowest below the mean lake water level was −6.455 m (Finol & Sancevic, 1995), up to −4 m since 1932 (Walford, 1995), up to −7 m between 1926 and 2004 (Chrzanowski, 2006), to up to −6.4 m with rates of 26 cm/yr (Murria, 2007), in areas of intensive oil production.

COLM is tectonically controlled by active faults such as the Icotea fault, with displacements on the order of 10 meters (ANIH, 2024), and by the Pueblo Viejo fault, whose deformation could affect the integrity of the dyke system. At the same time, the area has formations from the Pleistocene-Holocene to the Eocene, formed by alluvial and deltaic deposits (clays, silts, and sands) of the Catatumbo River and other tributaries, which are soft and compressible sediments. While urban and industrial surface loads drive progressive, irreversible sediment compaction, their anthropogenic surface settlements contribute far less, at a millimetric scale, to overall subsidence than the compaction caused by fluid extraction (Murria, 1991; Finol et al., 1995).

Due to the lithological characteristics of the area, it was necessary in 1932 to begin the design and construction of a protection system consisting of a land containment dyke, internal diversion dyke, and a drainage system (Murria, 1991, 2007), to prevent flooding in the areas occupied by the population and by oil activity. Currently, these areas lie about 5-6 m below lake level, cover 113 km^2 (11 300 hectares), and are home to around 100 000 inhabitants (ANIH, 2024).

By 1926, commercial oil exploitation began in the Lagunillas field. Only three years later, in 1929, observations of permanent flooding in the production areas raised suspicion of subsidence in the field, prompting a preliminary monitoring scheme. As exploitation continued to expand into neighboring areas, studies had to expand both onshore and offshore. From 1929 to 1987, a scheme was established by MARAVEN (a former national oil affiliated company) to monitor the subsidence process through the use of geodetic leveling, whose leveling network entailed 1436 benchmarks that covered the area between Tia Juana and Bachaquero, achieving accuracies of 20-30 mm (with 95% confidence) for the determination of subsidence (Walford, 1995) (see Figure 1).

The maximum subsidence rate, according to Murria (1991) and Finol et al. (1995), reached approximately 20 cm/yr, and maximum cumulative subsidence up to March 1990 reached 5 m in Lagunillas. In Tia Juana and Bachaquero. Subsidence reached maximum values of −4.462 m and −4.470 m, with maximum rates of 8 and 7 cm/yr, respectively, up to March 1988. The Cabimas and Mene Grande fields have remained stable to date. Rates range from 5 cm/yr along the coast between 1929 and 1990 (Murria, 1991; Finol & Sancevic, 1995), and the maximum accumulated subsidence rate found along the coastal dyke has been 7 cm/yr in the Lagunillas area (Murria, 1991), monitored during 1986-1988 using a network of 306 platform benchmarks; elevations were established relative to Mean Lake Water Level. Subsidence was calculated by comparing elevations between consecutive surveys. The historical record includes benchmark elevations, biannual relative subsidence, and total cumulative subsidence since oil exploitation began in 1928, covering 60 years through 1988.

In recent years, the Venezuelan oil industry has suffered the severe consequences of an ongoing political and economic crisis, leading to the emigration of highly skilled professionals, the gradual deterioration of infrastructure, and cyberattacks targeting institutional servers, among other impacts. These factors have severely constrained data accessibility beyond historically published studies, preventing direct comparison with concurrent operational datasets. Within this context, this paper evaluates, models, and projects the dynamics of oil-induced land subsidence along the Eastern Coast of Lake Maracaibo (COLM) by integrating DInSAR data, a 3D Volumetric Strain Model, and Deep Learning algorithms. Specifically, the InSAR-SBAS method is employed for the 2018–2022 period to estimate line of sight (LOS) displacement rates and decompose motion vectors into vertical (dU) and east-west (dE) components across three major oil fields. Furthermore, subsurface volumetric deformation is modeled using a 3D inversion algorithm (DTerrain) to

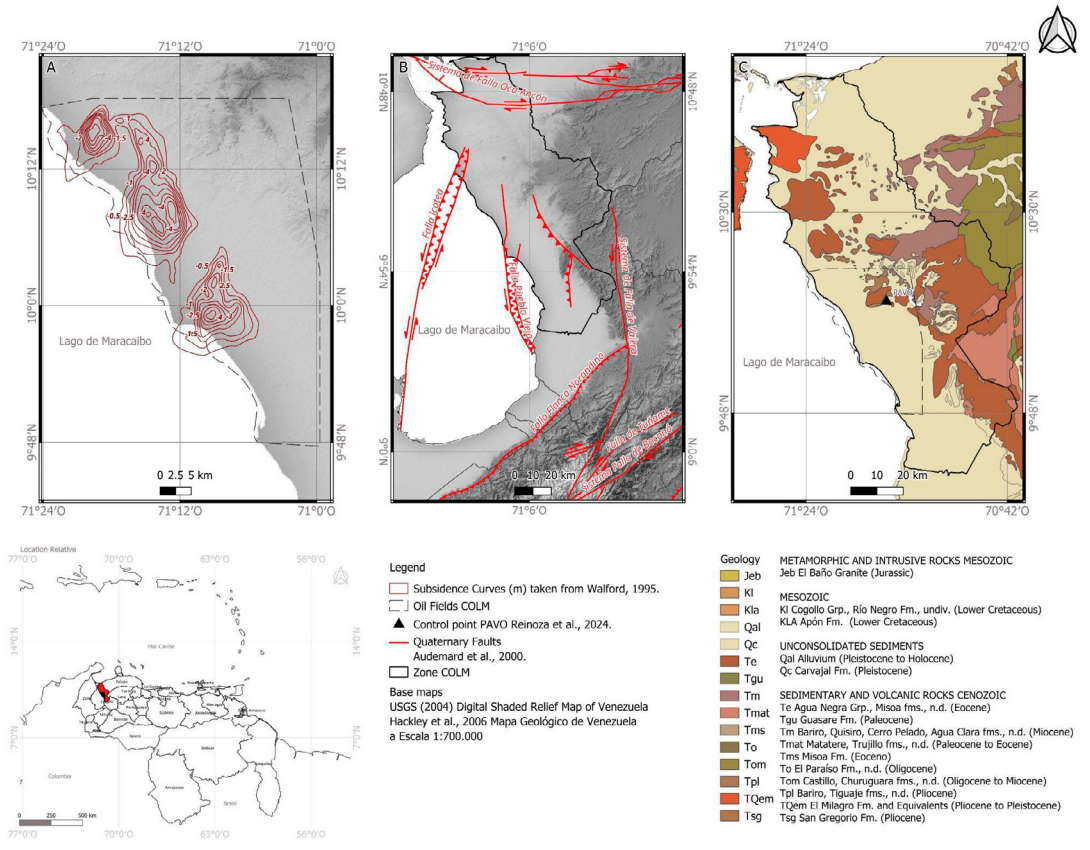


Figure 1. (A) The geodetic levelling network shows accumulated subsidence between 1929 and 1987 (modified from Walford, 1995). (B) Active fault systems of the East Coast of Lake Maracaibo (in black). Oca-Ancón (right lateral), Pueblo Viejo (reverse sinistral), Valera (sinistral), Mene Grande (reverse), Icotea (reverse), Flanco Norandino (inverse), Boconó (dextral) (Audemard et al., 2000, 2006). (C) Geology of the East Coast of Lake Maracaibo-COLM (in black; taken from Hackley et al., 2006).

identify the compaction depths and volumes responsible for surface subsidence. Additionally, a predictive model based on Long Short-Term Memory (LSTM) recurrent neural networks is constructed to forecast the temporal evolution of subsidence in the short and medium term (2023–2027). Ultimately, this work provides a robust technical framework for risk assessment and the protection of critical infrastructure along the COLM dike system.

1.1. Previous Studies with InSAR

In terms of SAR Satellite Interferometry, COLM area has been studied for almost two decades. Cano (2008) evaluated images from SAR ERS-1, ERS-2, and ENVISAT images to study ground subsidence in COLM; however, he did not obtain adequate coherence values to estimate displacement. Deguchi and Narita (2015), using PALSAR data in Fine Beam Single polarization (FBS) and ScanSAR modes through InSAR time series analysis, estimated soil deformations in the vicinity of three sites (Tia Juana, Lagunillas, and Bachaquero), with annual vertical displacement velocity values of −5.1 cm/yr, −10.3 cm/yr, and −5.8 cm/yr, respectively. Using SENTINEL-1 images, Arenas et al. (2019) obtained vertical movements between 2.8 cm/yr and −2.8 cm/yr in Cabimas, Tia Juana, and Ciudad Ojeda between 2014 and 2017. Quintana, 2021; Quntana-Sánchez et al., 2025) using SENTINEL-1 images, estimated the displacement in the direction of light of sight-LOS, in its ascending mode,

obtaining values of −4.0 cm in the Lagunillas area, 4.5 cm/yr in Ciudad Ojeda, Tia Juana with 3.5 cm/yr, Bachaquero with areas that rise towards the center of the city with 3.0 cm/yr and areas towards the NW with −2.0 cm/yr for a period between 2018-2019. Chávez (2023) used SENTINEL-11 images to derive mean strain velocities in ascending and descending SW directions, with rates up to −5.0 cm/yr and accumulated East-West displacement ranging from −8.0 cm to 8.0 cm. It highlights an accumulated vertical displacement in the Tía Juana and Lagunillas oil fields, with rates of −3.0 cm/yr and −4.0 cm/yr, respectively. It identified a significant concentration of Permanent Scattering (PS) in the Lagunillas Field, indicating considerable subsidence over much of the area, unlike the other adjacent oil fields. A rate displacement of more than 0.5 cm/yr spans 2015-2022, with accumulated subsidence of approximately 30 cm. González et al. (2024a), using TerraSAR-X images during the period 2011-2015, calculated an average subsidence rate of −3.5 cm/yr in the offshore Lagunillas Inferior 07 (LGINF-07) reservoir, allowing updating geomechanical models and understanding ground movements. González et al. (2024b) using TerraSAR-X images during the period 2011 - 2015, estimated the highest subsidence rate in the AGUA-230, AGUA-241 and AGUA-242 oil plots, within which there are a total of 193 wells, 1 flow station, 5 gas manifolds, 3 production manifolds and one high-pressure manifold, with subsidence velocities greater than or equal to −4.0 cm/yr and with an accumulated subsidence greater than or equal to −1.3 m, located in the U.P. Lagunillas Lago offshore.

1.2. Geological context

The Tia Juana, Lagunillas, and Bachaquero fields belong to COLM, which is morphologically limited to the west by Maracaibo Lake, to the south by the Andes Mountains, and to the east by the Trujillo Mountain range. It is surrounded by 6 active faults, which make it a tectonically active zone, such as the Oca-Ancón (right lateral), Pueblo Viejo (reverse sinistral), Valera (sinistral), Mene Grande-Burro Negro (reverse), Icotea (reverse), Flanco Norandino (reverse), and Boconó (dextral) faults (Audemard et al., 2000, 2006) (see Figure 1).

Quaternary active faults, such as the Pueblo Viejo and Burro Negro faults, cross the zone. Pueblo Viejo exhibits ~0.5 mm/yr of reverse sinistral slip (Vertical→Horizontal), while the Burro Negro fault has been catalogued only as reverse with a slow slip rate of 0.01 mm/yr (Audemard, 2001; Audemard et al., 2000; Beltrán, 1993; Soulas, 1986).

Geologically and geomorphologically, the oil fields lie in an old lacustrine environment, flat and swampy, just above the lake level. The area is predominantly composed of unconsolidated sediments, such as sand, silt, and alluvium, classified as Qal and Qc units within the Pleistocene-Holocene Carvajal Formation (see Figure 1). These marshes were separated from the lake by a relatively narrow strip of land elevated slightly above the lake's water level (Murria, 1991; Finol & Sancevic, 1995; Hackley et al., 2006).

2. Methodology

2.1. InSAR data collection and processing

To estimate the current deformation rates in COLM, the Differential Interferometric Synthetic Aperture Radar (DInSAR) technique was used, applying the Small Baseline Subset (SBAS) method based on an adequate combination of differential interferograms produced by data pairs characterized by a small orbital separation (baseline), keeping the phenomena of spatial decorrelation to monitor the evolution of the deformations of the Earth's surface to a minimum. To obtain the deformation values of this dataset, we used a maximum baseline of 200 m and a coherence of 0.5. We generated non-consecutive pairs using three combinations (instead of only consecutive pairs), which improved accuracy when averaging atmospheric errors, increased temporal resolution, and added redundancy to validate results.

A total of 280 Sentinel-1 interferometric images (145 in ascending orbits and 135 in descending orbits) were processed, with a temporal

resolution of 12 days, to estimate the subsidence rate from January 2018 to December 2022. The Sentinel-1 dataset acquisition was bound to the 2018–2022 period to maintain temporal and spatial coherence consistency. Following the end of the Sentinel-1B mission in December 2021, image acquisition intervals shifted from 6 days to 12 days. Standardizing the baseline network to this window ensured a uniform sampling frequency and optimal interferometric coherence across all three oil fields.

We implemented multiple combinations of non-consecutive pairs, generating 822 interferometric pair combinations. We used the PAV0 site of the FUNVISIS geodetic observation network as a reference point (Reinoza et al., 2024). This benchmark lies on a stable outcrop of Pliocene rocks (Reinoza et al., 2015). The velocity uncertainty values were computed using the standard error of the linear velocity estimation implemented in MintPy (Yunjun et al., 2019). This approach calculates the standard deviation of the displacement rates at each pixel level through a weighted least-squares approach on the unwrapped time series, effectively accounting for phase noise, residual atmospheric artifacts, and temporal decorrelation.

We processed and generated the interferograms in the InSAR Scientific Computing Environment (ISCE), currently funded by the NASA-ISRO SAR (NISAR) project. This environment was built in Python, which uses The Sentinel-1 TOPS stack processor algorithm (Fattahi et al., 2016) to generate the time series, with scripts supporting processing of Sentinel-1 TOPS image stacks. Currently supported workflows include an orbitally corrected SLC stack, co-registered using NASA's 1 arc sec (30 meters) NASA *Shuttle Radar Topography* Mission-SRTM Digital Elevation Model, interferogram networking, topographic phase removal, offset and coherence calculation, and phase unwinding using SNAPHU (Statistical-cost, Network-flow Algorithm for PHase Unwrapping) (Chen & Zebker, 2002).

For time-series analysis, we used InSAR MintPy (Miami InSAR Time-series software in Python) (Yunjun et al., 2019), which employs Small Baseline Subset (SBAS) inversion algorithms (Berardino et al., 2002). For atmospheric correction, PyAPS (Jolivet et al., 2011) was used to estimate differential phase delay maps (ramps) due to the stratified atmosphere, thereby correcting radar interferograms. It was rewritten in Python 3 from the PyAPS source code and adapted for ECMWF ERA-5 corrections by Yunjun et al. (2019).

2.2. 3D Volumetric Strain Inversion in Lagunillas Field

Lagunillas oil field shows the fastest rates of subsidence. Thus, we selected it to apply the 3D volumetric strain inversion, obtained for the 2018-2022 period from the InSAR-SBAS dataset. We geocoded the data using radar geometry and then corrected them geometrically in Python.

The 3D volumetric inversion was carried out using the DTerrain algorithm (Gallardo et al., 2025a), employing a conjugate gradient optimization scheme to solve the inverse problem based on 44 226 displacement observations and five displacement components defined through their directional cosines, enabling integration of multi-geometry measurements. We adopted a Poisson's ratio of 0.25, consistent with the mechanical behavior of unconsolidated to weakly consolidated sedimentary formations in the study area. The model domain was discretized into a three-dimensional grid of $100 \times 100 \times 150$ cells (east–west, north–south, and vertical). Forward modelling and Jacobian calculations were performed on a finer sampling grid of 501×501 nodes. Regularization was implemented with a damping factor (α) of 10^3 to balance data misfit and model smoothness, mitigating instability due to noise and the inherent ambiguity of inversion. The iterative solution was constrained to a maximum of 1000 iterations, with convergence achieved at a normalized misfit threshold of 10^{-3}, providing a stable, physically consistent estimate of subsurface volumetric strain distribution.

In this approach, volumetric strain is an inversion model parameter and is not calculated directly as the ratio between vertical surface displacement and the thickness of a deformable layer. The subsurface model is discretized into three-dimensional cells, and DTerrain estimates

the volumetric strain associated with each cell by solving the inverse relationship between subsurface volume changes and the observed surface displacement components. The resulting strain values are dimensionless and are reported here as microstrain per year (μstrain/yr), where negative values indicate volumetric contraction. We apply regularization to obtain a stable, spatially smooth solution to this inherently non-unique inverse problem. Consequently, the inversion does not require an assumed deformable-layer thickness or a deformable soil thickness map.

Preliminary parameter testing was performed with different damping and Poisson's ratio values before selecting the final inversion parameters. These tests produced broadly comparable spatial distributions of the principal volumetric contraction zone, although the magnitude and smoothness of the recovered strain varied. We adopted $\nu = 0.25$ and $\alpha = 10^3$ as a compromise between solution stability, data fit, model smoothness, and geological interpretability.

Because we did not retain the complete numerical outputs of these preliminary tests, we do not present a quantitative sensitivity assessment, and the absolute strain magnitudes should be interpreted with this limitation in mind.

2.3. Long Short-Term Memory (LSTM)

Finally, the Long Short-Term Memory (LSTM; Brownlee, 2022) algorithm was applied, a type of deep learning architecture specifically designed to handle time series, whose memory cell allows it to remembering information from previous time steps, ideal for the study area, where today's subsidence depends on the reservoir pressure and cumulative extraction from months or years ago. In addition, the algorithm can handle nonlinear data, where factors such as changes in the rate of fluid extraction or injection create complex patterns that the LSTM can learn better than linear models.

Using the LSTM network for a regression framework (adapted from Machine Learning Mastery), subsidence rates for the Lagunillas oil field were derived from InSAR-SBAS data for the 2018-2022 period. The implementation involved customizing the workflow for InSAR data loading, normalization, and missing value management. To ensure numerical stability during training, the LSTM model incorporated gradient clipping, ultimately achieving robust performance with a Root Mean Square Error (RMSE) of 0.01 on both training and testing sets. The model architecture used a look-back window of 12, leveraging the previous 12 measurements to forecast subsequent values, with a 77% train-size split; configured via tensorflow.keras.optimizers, a gradient clipping threshold of 1.0 was applied to mitigate NaN loss issues. This setup generated future deformation projections (m) for the 2023-2027 period.

3. Results

The values of displacement velocities obtained in the direction of view of the LOS sensor (in its ascending mode) were -2.62 ± 0.19 cm/yr in Tia Juana; -5.35 ± 0.12 cm/yr in Lagunillas; and -7.19 ± 0.29 cm/yr in Bachaquero (See Figures 2 and 3). The uncertainty values (± 0.19, ± 0.12, ± 0.29 cm/yr) are extremely low compared to the measured signals, indicating a high reliability in the results.

The estimated LOS rates in descending mode were -2.57 ± 0.15 cm/yr in Tia Juana; -5.91 ± 0.10 cm/yr in Lagunillas; and -2.05 ± 0.24 cm/yr in Bachaquero, indicating subsidence across all three fields. Note the highest subsidence rate in Lagunillas at -5.91 cm/yr (Figures 4 and 5). The different uncertainty values for each field remain low (± 0.15, ± 0.10, ± 0.24 cm/yr).

To obtain the deformation values in the east and vertical components, the data obtained for both modes of upward and downward trajectories were combined, using MintPy's asc_desc2horz_vert.py algorithm (Yunjun et al., 2019) that processes LOS velocity values in ascending and descending mode to derive horizontal (east-west) and vertical (up-down) deformation signals (see Figures 6-7). The deformation across the three fields is not homogeneous in extent. Nonetheless, Table 1 shows results at the three points selected to compare LOS velocities and deformation rates (black crosses in Figures 2, 4, 6, and 7), with Lagunillas as the

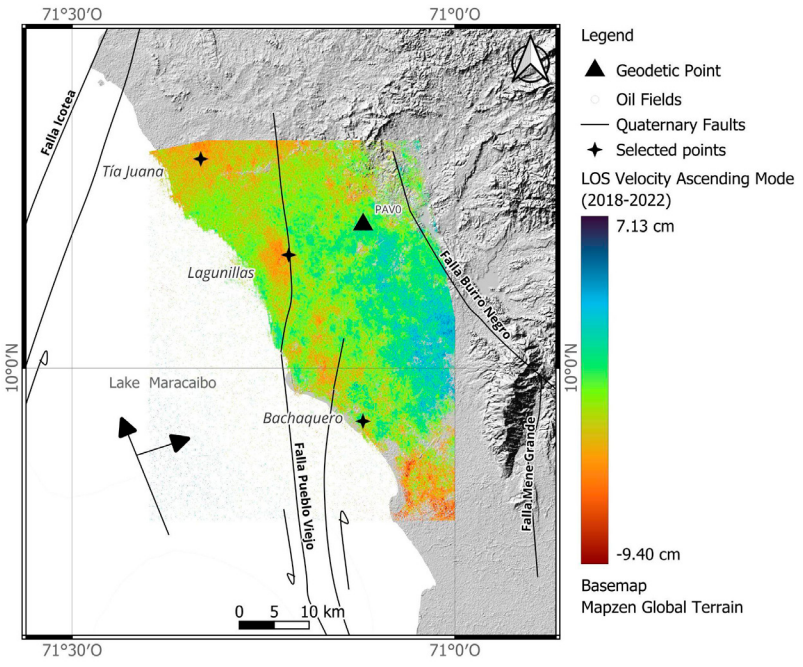


Figure 2. LOS Velocities Map for ascending mode during the period from January 2018 to December 2022. This map was generated from 422 interferogram pairs derived from 145 SLC Sentinel-1 images, with subsidence zones shown in red and the relatively stable zone in green. A standard deviation of 0.44 mm/yr indicates high precision and stability across the reference area. This confirms that phase-unwrapping errors, residual atmospheric artifacts (after PyAPS/ERA-5 corrections), and noise in the high-coherence pixels surrounding the PAV0 reference point (black triangle) are negligible relative to the large subsidence signals being monitored in COLM.

clearest case of predominantly vertical subsidence (-7.1 cm/year) among the three fields. Although both geometries (ascending and descending) showed negative rates (−5.35 cm/yr and −5.91 cm/yr), the difference between LOS and dU values may reflect a slight horizontal component or the different geometric sensitivities of each mode in the zone of maximum deformation. However, it remains the area of greatest subsidence. At the same time, Tia Juana and Bachaquero show significantly lower vertical rates (−4.5 cm/yr and −5.7 cm/yr, respectively) but still indicate active subsidence.

The high horizontal to vertical deformation ratio observed in Lagunillas aligns well with case studies in shallow, unconsolidated deltaic sediments. Furthermore, it is subject to intensive fluid extraction, such as the Wilmington oil field-Southern California, USA (35% to 45%) where values exceed classical elastic predictions due to the low shear modulus (G) and high compressibility of intercalated clay formations undergoing inelastic shear strain (Mayuga & Allen, 1969).

These high horizontal values are further driven by steep vertical subsidence gradients along the flanks of the depression and geotechnical boundary constraints imposed by the coastal dike infrastructure (Murria, 1991). Furthermore, the absence of a symmetric E-W pattern is attributed to the spatial superposition of adjacent fields from the neighboring Tía Juana and Bachaquero fields, additionally modified by a background regional tectonic strain component associated with active faulting in the Lake Maracaibo basin (Audemard et al., 2000) .

This deformation pattern is typical of subsidence induced by fluid extraction. Compaction of deep deposits not only causes vertical subsidence of the upper layer but also generates stresses that cause the surrounding ground to

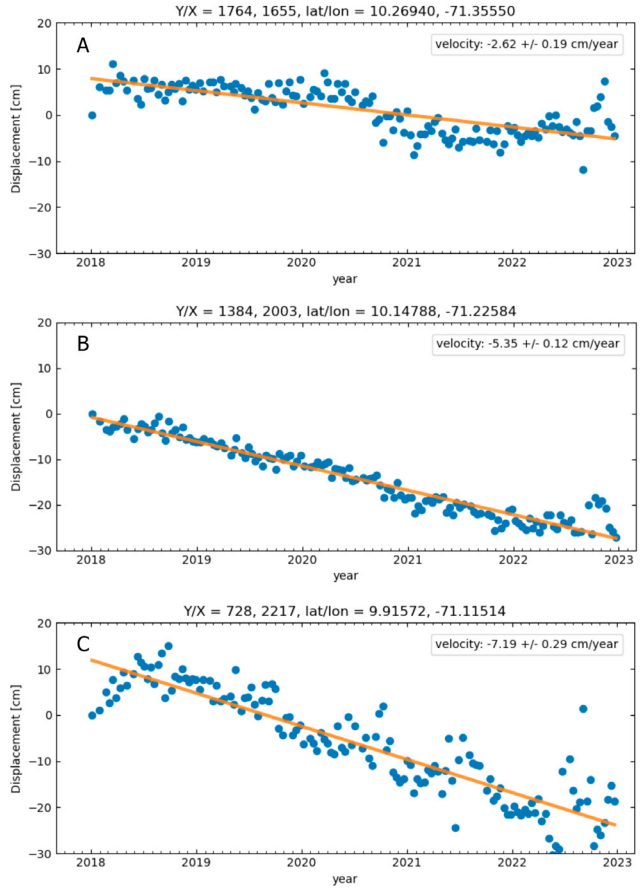


Figure 3. Displacements in LOS (cm/yr) in ascending mode from January 2018 to December 2022 for the Tia Juana (A), Lagunillas (B), Bachaquero (C) fields. (See location represented by a black star in each field in Figure 2). The Y/X values (radar coordinates) and lat/lon values (geographic coordinates) correspond to the acquisition point represented in the graph.

slide gravitationally toward the center of the depression. The most critical deformation area in the region is the Lagunillas field, where the profile shown in Figure 8B indicates values greater than −7 cm/yr.

The volumetric calculation in the Lagunillas field shows values of −600 μstrain/yr, indicating severe volumetric contraction (see Figure 9). This means the volume of a particular cell decreased by 0.06%. Although it seems small, when you add up thousands of cells with that deformation, it is what produces centimeters or decimeters of subsidence on the surface. With a known depth of 1676 m for one of its fields (PDVSA staff, personal communication), the

Table 1. LOS velocity and deformation rate in the east and vertical components for COLM during 2018-2022 at three selected points.

Fields	Lat (°)	Lon (°)	LOS (ascending) cm/yr	LOS (descending) cm/yr	East-West Deformation (dE) cm/yr	Vertical Deformation (dU) cm/yr
Tía Juana	10.27	-71.36	-2.62 ± 0.19	-2.57 ± 0.15	2.35	-4.5
Lagunillas	10.15	-71.23	-5.35 ± 0.12	-5.91 ± 0.10	-2.13	-7.1
Bachaquero	9.92	-71.12	-7.19 ± 0.29	-2.05 ± 0.24	-1.97	-5.7

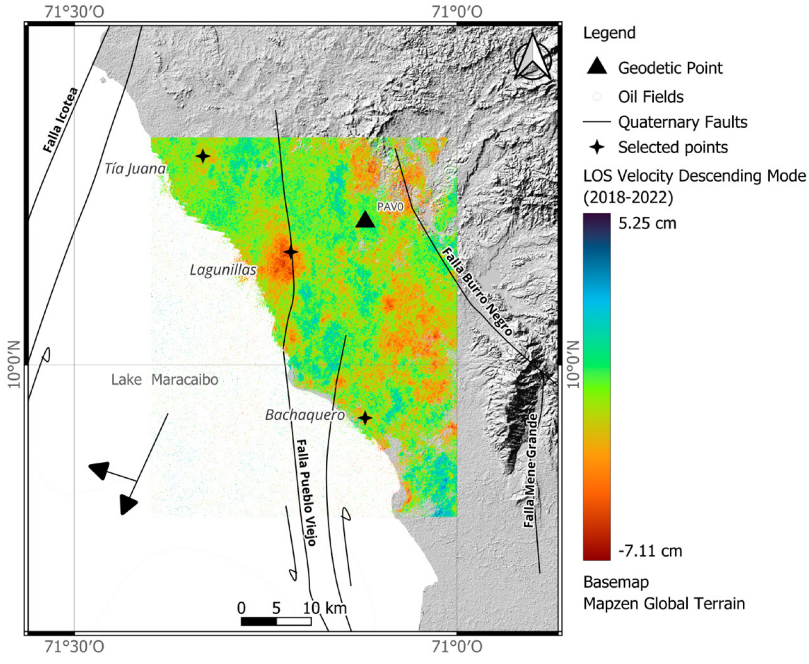


Figure 4. LOS Velocities Map for descending mode from January 2018 to December 2022. This map was generated from 399 interferometric pairs derived from 135 SLC Sentinel-1 images, with subsidence zones shown in red and the relatively stable zone in green. A standard deviation of 4 mm/yr is realistic, robust, and a standard uncertainty threshold for C-band Sentinel-1 InSAR time series over land subsidence areas. It reflects residual temporal noise, small uncorrected atmospheric variations, and local decorrelation across high coherence pixels relative to the stable PAV0 geodetic reference point (black triangle).

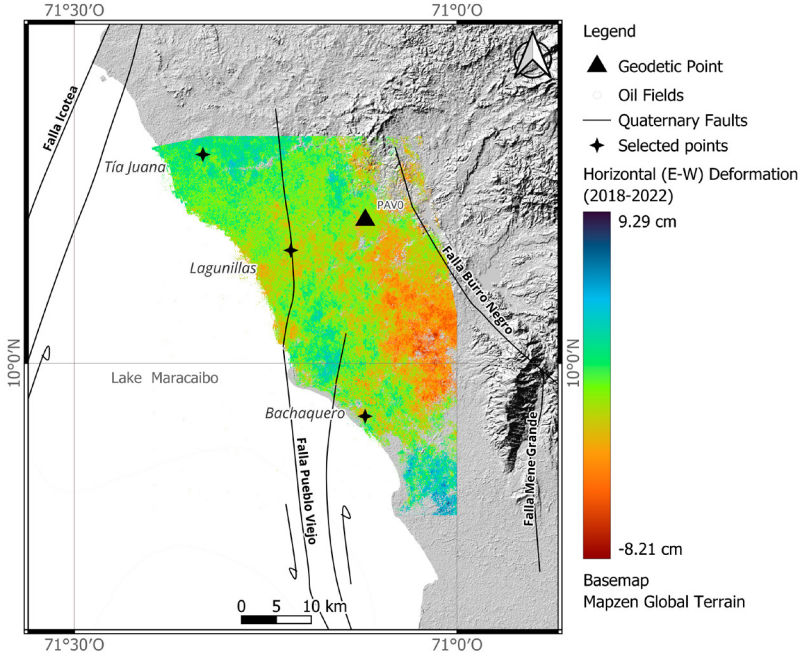


Figure 6. East-West deformation map for the period January 2018 to December 2022. This map is the product of combining both ascending and descending datasets.

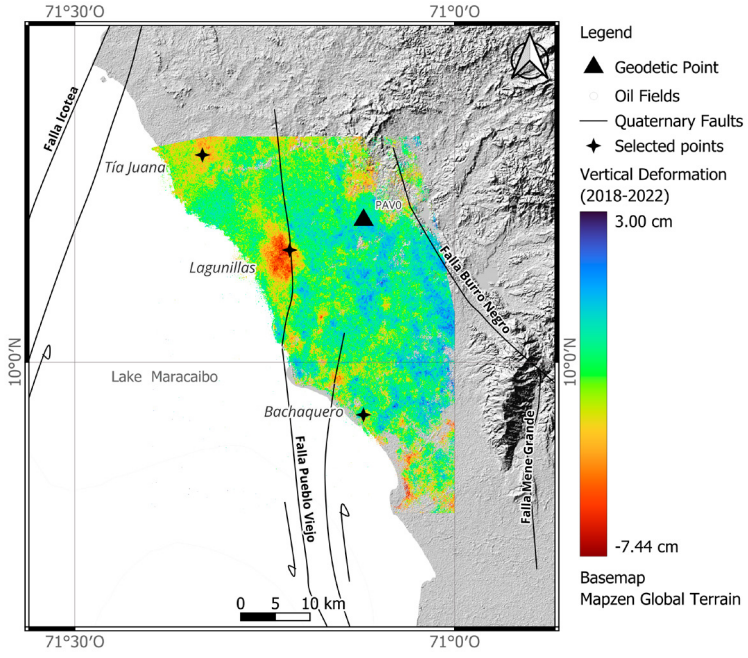


Figure 7. Vertical deformation map from January 2018 to December 2022. This map combines both ascending and descending datasets.

compaction is not superficial (soft soils) but occurs more than 1.5 km deep. It is not surface clay consolidation, but the effect of a pore-pressure drop in that specific layer. At that depth, compaction of sandstones or porous rocks that have lost fluid (water, steam, or oil) is likely. The estimated displacement (see Figure 9C) reflects the mathematical model of sinking based on the estimated strain values.

The model indicates a critical point in the area's stratigraphy, located in the Carvajal Formation (Miocene), which is known for its unconsolidated or poorly consolidated sands. When extracting crude oil, pore pressure drops and the sand's

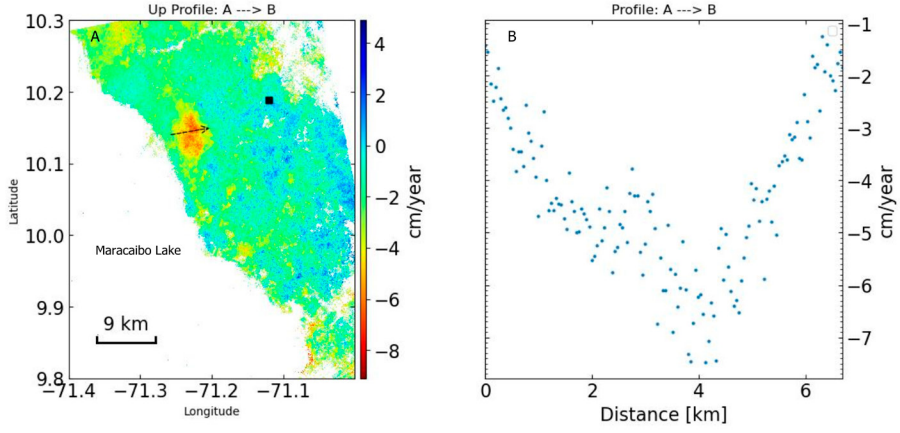


Figure 8. Vertical deformation profile (A) in the Lagunillas field for the period between January 2018 and December 2022. The profile (B) shows the subsidence with values greater than −7 cm/yr. The black square dot represents the PAV0 site of the FUNVISIS geodetic observation network (Reinoza et al., 2024).

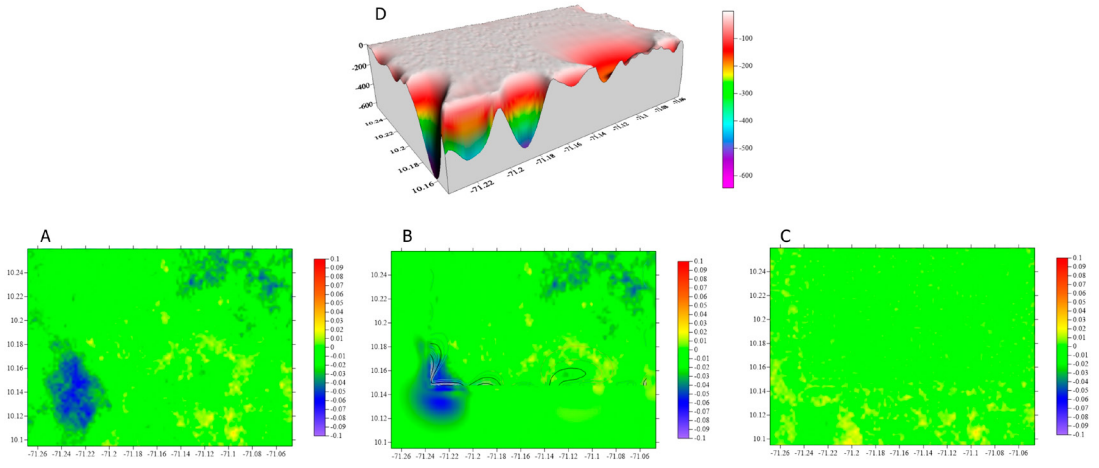


Figure 9. (A) Comparison of subsidence rates obtained from InSAR-SBAS for the period 2018-2022, (B) computed displacement from the 3D Volumetric Strain Model (Gallardo et al., 2025b), (C) the difference between subsidence rates and computed displacement and, (D) estimated strain values for the Lagunillas Oil Field.

mineral skeleton reorders (compacts); the value of −600 μstrain/yr measures that reordering at 1.6 km.

The resulting maps were jointly inverted to infer a deformation model that simultaneously compares and predicts deformation data. Ultimately, this enables precise identification of deep compaction zones, facilitating correlation between surface subsidence and oil extraction activities.

Applying LSTM in the Lagunillas field shows that current subsidence depends not only on extraction but also on the history of accumulated reservoir pressure. The relationship between oil extraction and subsidence is complex; applying LSTM to InSAR data allowed us to model these relationships. The projections estimated between 2023 and 2027 highlight the reservoir compaction processes (see Figure 10).

We loaded the deformation data from a CSV file and normalized it to a range between 0 and

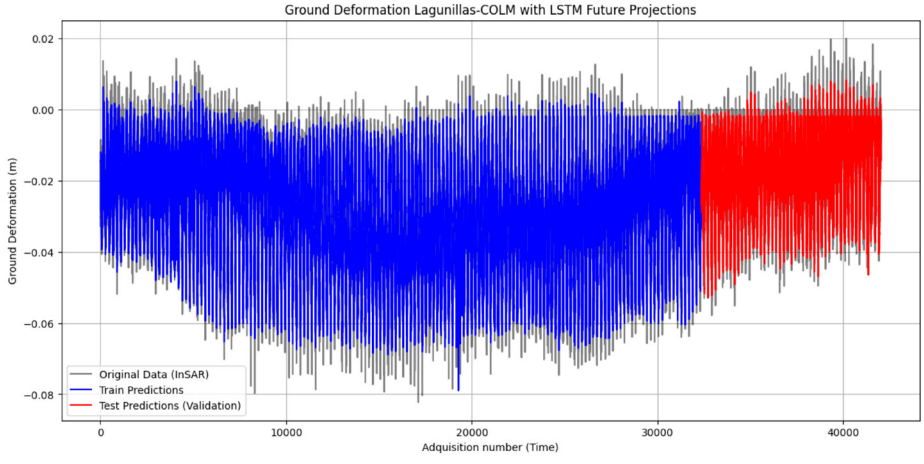


Figure 10. Ground deformation Lagunillas oil field COLM with LSTM future projections.

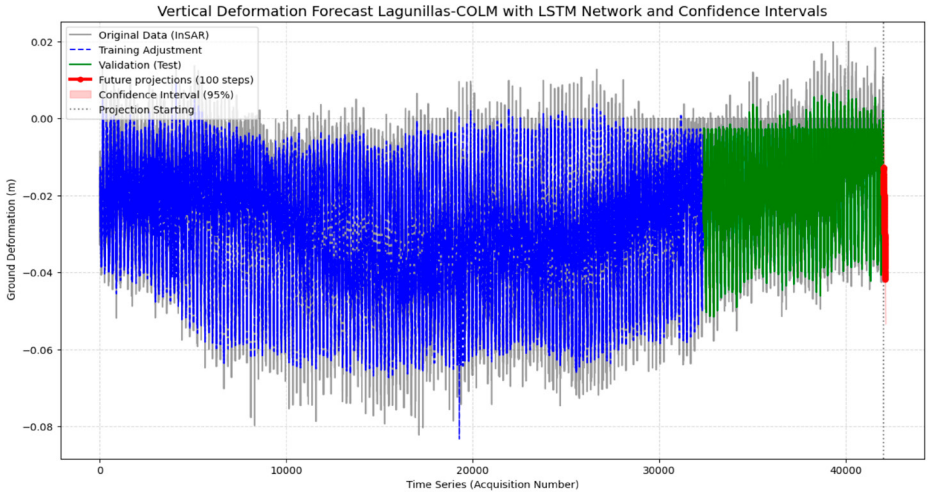


Figure 11. Ground deformation Lagunillas oil field COLM with LSTM Network and Confidence Intervals.

1 using MinMaxScaler to optimize neural network performance. The dataset was split into training (77%) and testing (23%) sets, applying an observation window (look_back = 12) to construct input sequences (trainX, testX) and target labels (trainY, testY). Under this setup, each model prediction relies on the preceding 12 measurements. We imputed any NaN values in the sequence sets with zeros to ensure numerical stability during training, and post-imputation checks confirmed no missing values remained.

A 32-neuron network was built and compiled with the Adam optimizer (clipvalue = 1.0) and mean_squared_error as the loss function. Training ran for 130 epochs with a batch size of 2. During training, the mean squared error progressively decreased, indicating that the model learned to fit the data.

Projections were applied over 100-time steps, equivalent to 4 years, showing deformation values in meters. The model achieved a root mean square error (RMSE) of 0.01 m in both training and testing, indicating that it fits both seen and unseen data well with very low error.

The results are shown in a graph that visualizes the original data, the training predictions, the validation (test) predictions, and the future projections (see Figure 10). Additionally, a 95% uncertainty band was included around the future projections, based on the test RMSE, giving a confidence range for the predictions (see Figure 11).

The generated graph (see Figure 12) shows that compaction persists for the 2023–2027 period (shown in red) based on the analyzed oil activity, with a projected deformation of −4 cm/yr. However, at the time of this study, the oil industry is reactivating across various fields in the country, raising the question: what will be the actual impact on subsidence in the Lagunillas area under this new operational scenario?

4. Discussion

The SBAS results for COLM's oil fields during 2018-2022 update the historical deformation pattern, predominantly subsidence, recorded since 1928. Consistent with the historical subsidence trend across the three oil fields, Lagunillas has the highest displacement rate, with a historical maximum of 20 cm/yr (Finol & Sancevic, 1995).

The InSAR data indicate that the subsidence process remains active more than 80 years after its onset. However, at rates of −7.1 cm/yr, substantially lower than the historical maximums recorded in Lagunillas (Murria, 1991; Finol & Sancevic, 1995). This deceleration suggests a possible evolution in the geomechanical response of the deposit or changes in exploitation

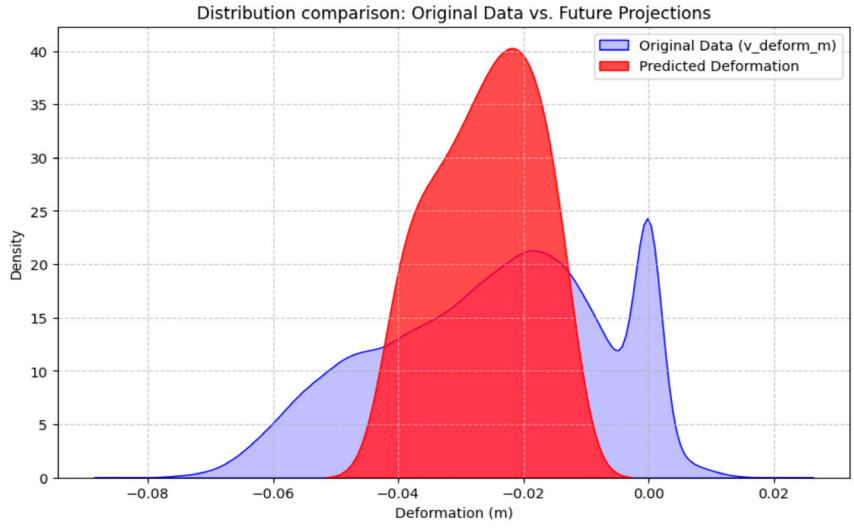


Figure 12. Comparison of original data vs. predicted deformation for the Lagunillas oil field.

practices, confirming that it is the epicenter or zone of maximum compaction of the reservoir. Here, vertical compaction is so great that it dominates any sign of horizontal movement.

The temporal evolution of InSAR displacement series reveals two distinct behaviors: a dominant long-term, non-linear downward trend driven by deep reservoir fluid extraction, and a secondary cyclic intra-annual signal. The main temporal variations in subsidence rates, characterized by intermittent periods of relative stabilization and accelerated settlement, qualitatively mirror historical operational fluctuations and production interruptions in the COLM fields. The seasonal cyclic oscillations are attributed to localized fluid injection schemes. From a poroelastic perspective, periodic fluid injection transiently increases pore pressure, reducing effective stress and triggering a minor, reversible poroelastic rebound that temporarily counteracts the ongoing inelastic consolidation of the reservoir.

The rates of annual displacement velocities in LOS and the values obtained for the east and vertical components in the main urban and oil production areas of Tía Juana, Lagunillas, and Bachaquero, reaching subsidence values of more than −7 cm/yr over 5 years, between 2018 and 2022, in the Lagunillas oil field, demonstrate that a process of sediment compaction continues due to the readjustment of the terrain.

The spatial distribution of oil fields and subsidence rates is correlated; the maximum subsidence values in the Lagunillas Field suggest it has the highest production density, validating the hypothesis that oil extraction is the main driver of land subsidence in COLM. Fluid removal reduces pore pressure in reservoirs, increasing effective stress and causing compaction of the producing layers and, consequently, surface subsidence.

The accumulated displacement of more than −7 cm/yr over 5 years in Lagunillas indicates that the area entails significant engineering and environmental risks, such as the integrity of the zone, which is more critical in Lagunillas, whose continuous subsidence reduces the level of protection of the containment dyke, that protects the coastal areas from flooding of the lake. InSAR data indicate subsidence of the Lagunillas dike, with deformation rates of about 4 cm/year in the vertical component and 3 cm/year in the horizontal component (see Figure 13).

Consequently, these depressed sectors face heightened vulnerabilities to potential flooding and damage to infrastructure, affecting the structural stability of buildings and roads, in

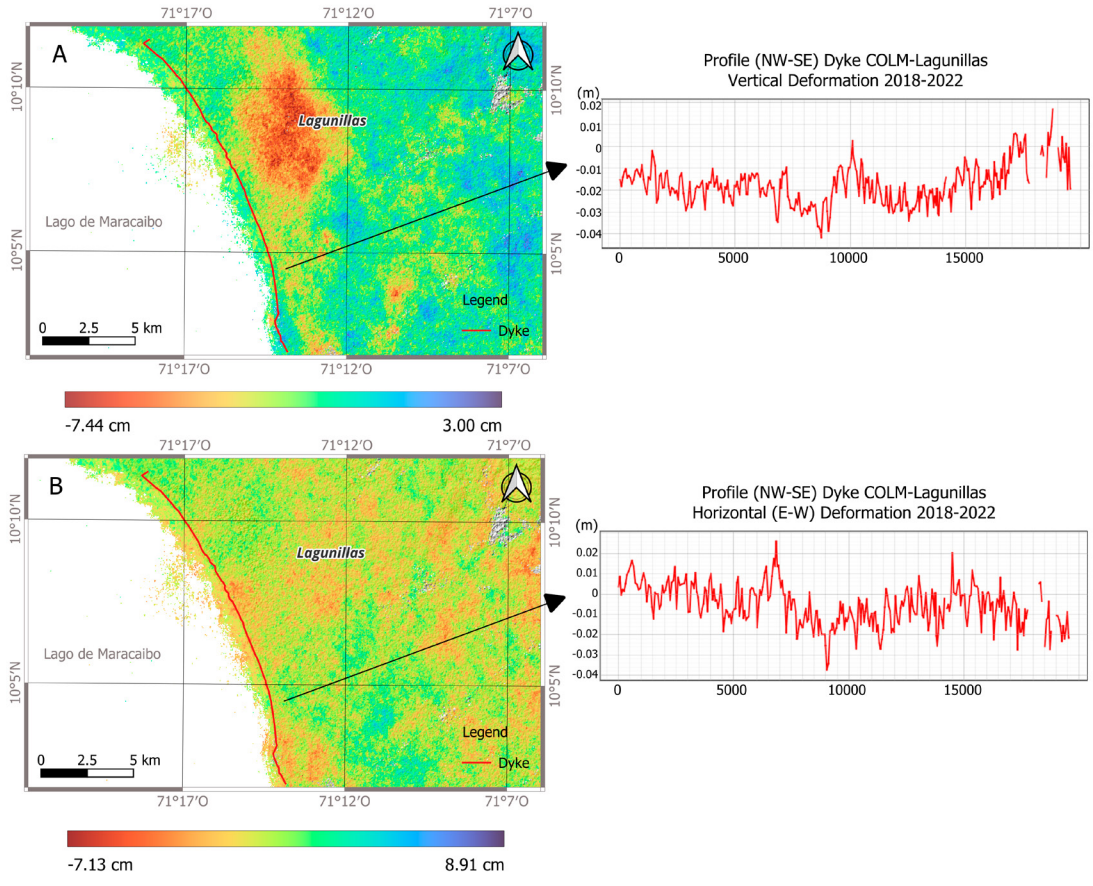


Figure 13. Average vertical (A) and horizontal (E-W) (B) deformation on the Lagunillas dyke to the period 2018-2022.

the most depressed areas. Geomechanical monitoring is critical to updating reservoir models, allowing the oil operators to adjust production and injection strategies to mitigate future compaction.

The causal mechanism linking subsurface compaction to surface subsidence is governed by pore-pressure drawdown within the unconsolidated, high porosity Miocene sandstone reservoirs. According to Terzaghi's effective stress principle (Terzaghi, 1943), a reduction in fluid pore pressure transfers the overburden load to the mineral skeleton, increasing uniaxial effective stress. Given the low shear moduli (G) and high uniaxial compressibility of the interbedding unconsolidated or poorly consolidated layers, this stress shift induces non-elastic, volumetric compaction. Based on the 3D strain inversion results (DTerrain) (Gallardo et al., 2025b) demonstrate that compaction at depths of 1.6 km transfers directly to surface vertical displacement (dU), where the depth to width ratio dictates the curvature and extent of the surface subsidence trough. The vertical gradients observed at the flanks of these compaction zones reflect localized stress concentrations near formation boundaries.

Given the limited nature of oil production data, the LSTM architecture was used to extract intrinsic temporal dependencies in InSAR deformation series. At the same time, the estimated volume allowed geolocating the compaction source at 1676 m, providing a physical interpretation of the predictive model. A key limitation of the present LSTM forecasting model is its reliance strictly on historical InSAR-derived deformation time series, operating as a univariate data-driven extrapolation. Consequently,

human induced operational variables, such as oil extraction rates, fluid injection volumes, and pore pressure changes, are not explicitly embedded within the predictive architecture. Under current conditions, where local oil operations are undergoing potential reactivation, changes in production regimes could alter future compaction dynamics in ways that a purely historical time-series model cannot anticipate. If operational datasets were available, a viable approach to overcome this limitation would be to implement a multivariate LSTM architecture that would represent a viable path forward.

Finally, it should be noted that the seismological and monitoring network of the dyke, which is used to monitor the subsidence process, is not currently operational. This situation raises concerns about a potential rupture, which would entail substantial human and economic losses (ANIH, 2024). Although land subsidence has transitioned into a slower, steadier phase compared to historical peaks, the deformation process remains fully active and continuous.

5. Conclusions

The active subsidence of COLM and the prevalence of the Lagunillas field as the most critical area are confirmed, evidencing a complex deformation process in which reservoir compaction causes vertical subsidence and horizontal sliding of the surrounding terrain toward its center.

Risk assessment requires monitoring this process, whose movement affects linear infrastructure such as pipelines and roads in ways distinct from mere vertical subsidence. Similarly, it is necessary to maintain the dike, roads, flow lines, and other surface facilities, such as those associated with residential areas in the Lagunillas area. Likewise, the risk of flooding resulting from the low topographic level relative to the lake in this area remains.

This study, using the InSAR-SBAS technique, has contributed to updating subsidence measurements in COLM for the selected period, which, together with previous InSAR studies, has helped clarify the terrain's current geodynamics.

Applying the DTerrain code linked surface displacements with compaction processes in the reservoir. The strain values (specifically the peak at 1676 m depth in Lagunillas, −600 μstrain/yr) suggest that subsidence directly responds to porosity deflation in the Miocene producing units.

The LSTM artificial intelligence model proved to be an effective tool for capturing the nonlinear nature of subsidence. The projection to 2027 enables risk-scenario anticipation, supporting preventive decision-making for maintaining containment dikes and drainage systems.

Combining the DTerrain code for 3D inversion with deep learning architectures for time series represents a significant advance over traditional methods, enabling continuous, autonomous monitoring in areas where access to internal oil production data is restricted.

Subsidence in COLM continues, a process driven by oil extraction and sediment compaction, and is projected to continue. However, as of the date of this study, a large-scale reactivation of the oil industry is beginning. We recommend continuing this type of study, which allows decision-makers and government entities to adopt best practices for public safety and well-being and for the recovery and protection of affected infrastructure.

Funding

The authors declare that no funds, grants, or other support were received during the preparation of this manuscript.

Author Contributions

All authors contributed to the study conception and design. Material preparation, data collection, and analysis were performed by Gabriela Quintana-Sánchez, Carlos Reinoza, Franck Audemard, Fikret Dogru, Gareth Funning, and Fredy Díaz-Mila. The first draft of the manuscript was written and the data was processed by Gabriela Quintana-Sánchez. The DTerrain code was processed by Fikret Dogru using TUBITAK ULAKBIM, High Performance and Grid Computing Center (TRUBA resources); all authors commented on previous versions of the manuscript. All authors read and approved the final manuscript.

Acknowledgments

This publication is part of the Gabriela Quintana Doctoral Program in Engineering Sciences at the Central University of Venezuela. The authors express their sincere gratitude to Eng. Luis Alejandro Jiménez (President) and Eng. María José Saavedra (Geophysics Department) from FUNVISIS. Thanks to PDVSA staff, including Eng. Hydio Conrado, Superintendent of Specialized Studies (Dikes & Drainage Management, COLM Division, West Production), and Eng. Carmen Rothe, Geodesy, Metocean, and Geotechnics Manager (General Management of Geophysics & Geodesy), for their invaluable support. And finally thanks to Dr. Luis Gallardo from CICESE. The numerical calculations reported in this paper were partially performed at TUBITAK ULAKBIM, High Performance and Grid Computing Center (TRUBA resources). The authors express their sincere gratitude to the journal's editorial team and the anonymous reviewers for their valuable suggestions, which significantly contributed to improving the quality of this work.

References

Academia Nacional de la Ingeniería y el Hábitat (ANIH) (2024). Declaración de la Academia Nacional de la Ingeniería y el Hábitat sobre la Vulnerabilidad y Riesgos del Sistema de Protección de la Costa Oriental del Lago de Maracaibo. https://acading.org.ve/wp-content/uploads/2024/11/DECLARACION_PROTECCION_COSTA_ORIENTAL_LAGO_DE_MARACAIBO.pdf

Arenas, I., Hernández, B., Royero, G., Cioce, V., & Wildermann, E. (2019). Detección de subsidencia por efecto de extracción petrolera aplicando la técnica DInSAR en Venezuela. *Revista Mapping, 28*(195). Available in: https://revistamapping.com/deteccion-de-subsidencia-por-efecto-de-extraccion-petrolera-aplicando-la-tecnica-dinsar-en-venezuela/

Audemard, F. (2001). Revisión y actualización de los parámetros sismogénicos de las fallas activas o potencialmente activas en Venezuela. *FUNVISIS'Unpublished Rpt for INTEVEP SA*, 24.

Audemard, F. A., Machette, M., Cox, J., Hart, R., & Haller, K. (2000). Map of Quaternary Faults of Venezuela. Scale 1:2,000,000. Map and Database of Quaternary Faults in Venezuela and Offshore regions (USGS Open-File Report 00-18, 78 p). A project of the International Lithosphere Program Task Group II-2: Major active Faults of the World (Regional Coord.: Carlos Costa, Univ. San Luis-Argentina, ILP II-2 co-chairman Western Hemisphere: Michael Machette, USGS-Colorado).

Audemard, F. A., Singer, A., Soulas, J. P., & the Neotectonics section of the FUNVISIS Earth Sciences Department. (2006). Quaternary faults and stress regime of Venezuela. *Revista de la Asociación Geológica Argentina, 61*(4), 492-503.

Beltrán, C. (1993). Mapa Neotectónico de Venezuela, escala 1:2.000.000.

Berardino, P., Fornaro, G., Lanari, R., Sansosti, E. (2002). A new algorithm for surface deformation monitoring based on small baseline differential SAR interferograms. *IEEE Transactions on Geoscience and Remote Sensing, 40*(11), 2375–2383. https://doi. org/10.1109/TGRS.2002.803792

Brownlee, J. (2022). Time Series Prediction with LSTM Recurrent Neural Networks in Python with Keras. *Machine Learning Mastery Blog*, article online: https://machinelearningmastery.com/time-series-prediction-lstm-recurrent-neural-networks-python-keras/

Cano, V. (2008). *Potential of SAR Interferometry for studying Land Subsidence due to Petroleum Extraction in East Coast of Maracaibo Lake, Venezuela* (Diploma course). Indian Institute of Remote Sensing (IIRS), National Remote Sensing Agency (NRSA), India.

Chávez, N. (2023). *Control de las deformaciones recientes del terreno producidas por la extracción de petróleo en la Cuenca del Lago de Maracaibo (Venezuela) utilizando técnica InSAR multi-temporale*s. Trabajo Especial de Grado. Universidad de Jáen. España.

Chen, C. W., Zebker, H. A. (2002). Phase unwrapping for large SAR interferograms: Statistical segmentation and generalized network models. *IEEE Transactions on Geoscience and Remote Sensing, 40*, 1709-1719. https://web.stanford.edu/group/radar/softwareandlinks/sw/snaphu/

Chrzanowski, A.S., Chrzanowski, A., Ortíz, E. (2006). *Modeling of ground subsidence in oil fields*. Technical Sciences. Canadian Centre for Geodetic Engineering (CCGE), University of New Brunswick. Canada. https://uwm.edu.pl/wnt/technicalsc/ts9_2006/13_9_2006.pdf

Deguchi, T., & Narita, T. (2015). Monitoring of land deformation due to oil production by InSAR time series analysis using PALSAR data in Bolivarian Republic of Venezuela. In *Proceedings of FRINGE'15: Advances in the Science and Applications of SAR Interferometry and Sentinel-1 InSAR Workshop*. Frascati, Italy: ESA Publication SP-731. http://proceedings.esa.int/files/331.pdf

Díaz-Mila, F., Escobar-Rey, L. K., & Mora-Páez, H. (2025). Análisis cuantitativo de la subsidencia en la zona suroccidental de la Sabana de Bogotá mediante geodesia InSAR. *Revista de Teledetección, 65*, 21345. https://doi.org/10.4995/raet.2025.21345

Fattahi, H., Agram, P., & Simons, M. (2016). A Network-Based Enhanced Spectral Diversity Approach for TOPS Time-Series Analysis, *IEEE Transactions on Geoscience and Remote Sensing, 55*(2), 777-786, https://doi.org/10.1109/TGRS.2016.2614925.

Finol, A., & Sancevic, Z.A. (1995). Subsidence in Venezuela. Chapter 7. Subsidence due to Fluid Withdrawal. In *Developments in Petroleum Science, 41*. Elsevier. https://doi.org/10.1016/S0376-7361(06)80054-3

Gallardo, L., Sarychikhina, O., & Glowacka, E. (2025a). DTERRAIN: 3D inverse modeling of InSAR and surface displacement data, *Mendeley Data, V1*, https://doi.org/ 10.17632/sbj87sjzf3.1

Gallardo, L., Sarychikhina, O., Glowacka, E., & Robles, B. (2025b). 3D Volumetric Strain Distribution of the Cerro Prieto Geothermal Field Inferred from Inverse Modeling of InSAR and Leveling Data. *Geophysical Research Letters, 52*(e2025GL115316), 1-10. https://doi.org/ 10.1029/2025GL115316

Galloway, D.L., Burbey, T.J. (2011). Review: Regional land subsidence accompanying groundwater extraction. *Hydrogeol. J. 19*, 1459–1486. https://doi.org/10.1007/s10040-011-0775-5

González-Freites, D. A., Zambrano-Mendoza, O., Barrios, J. L. (2024a). DInSAR para Análisis Geomecánico de Yacimientos – Aplicación al Yacimiento Lagunillas Inferior 07, Lago de Maracaibo, Venezuela. *Rev. Téc. Fac. Ing. Univ. Zulia, 47*, e244708. https://doi.org/10.22209/rt.v47a08

González-Freites, D. A., Zambrano-Mendoza, O. y Barrios, J. L. (2024b). Comparación del Modelo Geomecánico obtenido a través de DInSAR con el Modelo existente generado a partir de Registros de Pozos para el yacimiento Lagunillas Inferior-07 (LGINF-07) en el Lago de Maracaibo, Venezuela, *Rev. Téc. Fac. Ing. Univ. Zulia, 47*, p. e244709. https://doi.org/10.22209/rt.v47a09

Hackley, P., Urbani, F., Karisen, A., & Garrity, C. (2006). Mapa Geológico de Venezuela a Escala 1:700.000. USGS-UCV. https://pubs.usgs.gov/of/2006/1109/

Jolivet, R., Grandin, R., Lasserre, C., Doin, M.-P., Peltzer, G. (2011). Systematic InSAR tropospheric phase delay corrections from global meteorological reanalysis data, *Geophys. Res. Lett., 38*, L17311, https://doi.org/10.1029/2011GL048757

Mayuga, M. N., & Allen, D. R. (1969). Subsidence in the Wilmington Oil Field, Long Beach, California, USA. In *Proceedings of Tokyo Symposium on Land Subsidence*, *1*, pp. 66-79. https://www.saveballona.org/gasoilfields/WilmSubGC.pdf

Murria, J. (1991). Subsidence Due to Oil Production in Western Venezuela: Engineering Problems and Solutions. *Land Subsidence* (Proceedings of the Fourth International Symposium on Land Subsidence, May 1991). IAHS Publ. no. 200, 1991. https://paperzz.com/doc/7845701/subsidence-due-to-oil-production-in-western-venezuela

Murria, J. (2007). Ground subsidence measuring, monitoring and modeling in the Costa Oriental Oilfields in Western Venezuela: the last fifty years. *8th International Conference "Waste Management, Environmental Geotechnology and Global Sustainable Development (ICWMEGGSD'07 - GzO'07)"* Ljubljana, SLOVENIA. http://www.srdit.si/gzo07/abstracts/15JMurria_abstr02.pdf

Murria, J., & Saab, J. A. (1992). Problems and solutions in emergency planning for Western Venezuela oilfields. Presented at the *Earthquake Engineering, Tenth World Conference*, Rotterdam. https://www.iitk.ac.in/nicee/wcee/article/10_vol10_5917.pdf

Quintana, G. (2021). *Estudio de las deformaciones de la corteza derivadas de la geodinámica a partir de la Interferometría SAR (Synthetic Aperture Radar): Ejemplos de aplicación (Kumamoto-Japón, Valencia y Costa Oriental del Lago de Maracaibo-Venezuela)*, Trabajo Especial de Grado. Universidad Central de Venezuela-UCV, Venezuela.

Quintana-Sánchez, G., Audemard, F., Reinoza, C., Dogru, F., & Alvarado, L. (2025). Estudio de las deformaciones de la corteza derivadas de la geodinámica a partir de la Interferometría SAR (Synthetic Aperture Radar): Aplicación a la Costa Oriental del Lago de Maracaibo-Venezuela. *Revista Cartográfica*, (110). https://doi.org/10.35424/rcarto.i110.5874

Reinoza, C., Audemard, F. A., Jouanne, F., & Beck, C. (2015). An overview of the GNSS Geodetic Measurements Applied to Geodynamic Studies in Venezuela. In Michael Schmitz, Franck Audemard, & Franco Urbani (Eds.), *El Límite Noreste de la Placa Suramericana – Estructuras Litosféricas de la Superficie al Manto* (pp. 323–335). Edición Innovación Tecnológica. Facultad de Ingeniería, Universidad Central de Venezuela, Fundación Venezolana de Investigaciones Sismológicas.

Reinoza-Gomez, C. E., Audemard-M., F. A., Pereira, R., Ortega, L., Schmitz, M., Yegres-Herrera, L. A., & Mora-Páez, H. (2024). Velocity field for Western Venezuela: Elastic modeling in the Southern Merida Andes. *Boletín Geológico, 51*(1). https://doi.org/10.32685/0120-1425/bol.geol.51.1.2024.672

Solano-Rojas, D., Cabral-Cano, E., Hernández-Espriú, A., Wdowinski, S., DeMets, C., Salazar-Tlaczani. L., Falorni, G., Bohane. A. (2015). La relación de subsidencia del terreno InSAR-GPS y el abatimiento del nivel estático en pozos de la zona Metropolitana de la Ciudad de México. *Boletín de la Sociedad Geológica Mexicana, 67*(2), 273-283. https://www.scielo.org.mx/pdf/bsgm/v67n2/v67n2a11.pdf

Soulas, J. P. (1986). Neotectónica y tectónica activa en Venezuela y regiones vecinas. *VI Congreso Geológico Venezolano*, 6961–6999.

Terzaghi, K. (1943). *Theoretical Soil Mechanics*. John Wiley & Sons, New York. https://doi.org/10.1002/9780470172766.fmatter.

Walford, J. (1995) *GPS Subsidence study of the Costa Bolivar oil fields, Venezuela*. Technical Report, N 174. Geodesy and Geomatics Engineering. University of New Brunswick. https://unbscholar.lib.unb.ca/items/f28b8a38-0710-4cbf-a353-38fde8a67663

Yunjun, Z., Fattahi, H., & Amelung, F. (2019), Small baseline InSAR time series analysis: Unwrapping error correction and noise reduction. *Computers & Geosciences, 133*, 104331. https://doi.org/10.1016/j.cageo.2019.104331